HHS Public Access

Author manuscript

Nat Biotechnol. Author manuscript; available in PMC 2017 July 17.

Published in final edited form as:

Nat Biotechnol. 2016 October ; 34(10): 1066–1071. doi:10.1038/nbt.3663.

Blood pressure regulation by CD4+ lymphocytes expressing choline acetyltransferase

Peder S. Olofsson[1,2], **Benjamin E. Steinberg**[2,3], **Roozbeh Sobbi**[4], **Maureen A. Cox**[3], **Mohamed N. Ahmed**[5], **Michaela Oswald**[6], **Ferenc Szekeres**[7,12], **William M. Hanes**[2], **Andrea Introini**[8], **Shu Fang Liu**[5], **Nichol E. Holodick**[9], **Thomas L. Rothstein**[9], **Cecilia Lövdahl**[7], **Sangeeta S. Chavan**[2], **Huan Yang**[2], **Valentin A. Pavlov**[2], **Kristina Broliden**[8], **Ulf Andersson**[10], **Betty Diamond**[11], **Edmund J. Miller**[5], **Anders Arner**[7], **Peter K. Gregersen**[6], **Peter H. Backx**[4,13], **Tak W. Mak**[3], and **Kevin J. Tracey**[2,10]

[1]Center for Bioelectronic Medicine, Department of Medicine, Solna, Karolinska Institutet, Karolinska University Hospital, Stockholm, Sweden

[2]Laboratory of Biomedical Science, The Feinstein Institute for Medical Research, Manhasset, NY, USA

[3]The Campbell Family Institute for Breast Cancer Research, University Health Network, Toronto, ON, Canada

[4]Division of Cardiology, Peter Munk Cardiac Centre, University Health Network, Toronto, Ontario, Canada

[5]Center for Heart and Lung Research, The Feinstein Institute for Medical Research, Manhasset, NY, USA

[6]Robert S. Boas Center for Genomics and Human Genetics, Feinstein Institute for Medical Research, Manhasset, NY, USA

[7]Department of Physiology and Pharmacology, Karolinska Institutet, Stockholm, Sweden

[8]Department of Medicine, Solna, Unit of Infectious Diseases, Center for Molecular Medicine, Karolinska Institutet, Karolinska University Hospital, Stockholm, Sweden

Corresponding author: Peder S Olofsson, Peder.Olofsson@ki.se.

Accession Codes

Data in process of submission #XXXX-XXXX

Author contributions

PSO and KJT conceived the study, planned and performed experiments, analyzed data and wrote the manuscript. UA, BD and TWM planned experiments and edited the manuscript. BES, WMH and MAC planned and performed experiments and analyzed data. MO and PGK planned experiments, analyzed gene expression and edited the manuscript. RS and PHB planned experiments, measured murine blood pressure, performed telemetry and echocardiography, and analyzed data. MNA and EJM planned, performed and analyzed experiments with endothelial cells in vitro and murine blood pressure in response to cell infusion. FS and AA planned, performed and analyzed experiments on murine blood pressure in response to cell infusion. AI, VAP, KB, HY, SSC, SFL, CL, TLR, NEH performed experiments and analyzed data.

Competing Financial Interests

The authors have no competing financial interests to declare.

[9]Center for Oncology and Cell Biology, The Feinstein Institute for Medical Research, Manhasset, NY, USA

[10]Department of Women's and Children's Health, Karolinska Institutet, Stockholm, Sweden

[11]The Center for Autoimmune and Musculoskeletal Diseases, The Feinstein Institute for Medical Research, Manhasset, New York, USA

[12]School of Health and Education, University of Skövde, Skövde, Sweden

[13]Department of Biology, York University, Toronto, Ontario, Canada

Abstract

Blood pressure regulation is known to be maintained by a neuro-endocrine circuit, but whether immune cells contribute to blood pressure homeostasis has not been defined. We previously described that $CD4^+$ T lymphocytes that express choline acetyltransferase (ChAT), which catalyzes the synthesis of the vasorelaxant acetylcholine, relay neural signals[1]. Here we show that these $CD4^+$ $CD44^{high}$ $CD62L^{low}$ T helper cells by gene expression are a distinct T cell population defined by ChAT (CD4 T_{ChAT}). Mice lacking ChAT expression in $CD4^+$ cells have elevated arterial blood pressure and echocardiographic assessment consistent with increased vascular resistance as compared to littermate controls. Jurkat T cells overexpressing ChAT (JT_{ChAT}) decreased blood pressure when infused into mice. Co-incubation of JT_{ChAT} increased endothelial cell levels of phosphorylated eNOS, and of nitrates and nitrites in conditioned media, indicating increased release of the potent vasodilator nitric oxide. The isolation and characterization of CD4 T_{ChAT} cells will enable analysis of the role of these cells in hypotension and hypertension, and may suggest novel therapeutic strategies by targeting cell-mediated vasorelaxation.

A major physiological mechanism of blood pressure regulation is through modulation of blood flow by alterations in vessel diameter. Acetylcholine, a signaling molecule produced by neurons and lymphocytes, is a vasorelaxant that decreases blood vessel resistance and reduces blood pressure[2]. Binding to cognate cholinergic receptors on endothelial cells, acetylcholine stimulates phosphorylation of endothelial nitric oxide synthase (eNOS), the rate limiting enzyme in the biosynthesis of nitric oxide (NO). Endothelium-derived NO diffuses into smooth muscle cells in the vascular wall, where it interacts with the heme-containing protein guanylate cyclase to induce synthesis of cGMP. This secondary messenger down-modulates availability of intracellular calcium required for myosin phosphorylation, leading to relaxation of vascular smooth muscle cells, and decreased blood pressure. Paradoxically, most arteries are innervated by adrenergic nerves and endothelial cells do not receive major direct input from acetylcholine-secreting neurons[3–5].

While studying the neural regulation of immunity, we previously identified a specific role for lymphocyte-derived acetylcholine in relaying neural signals in the inflammatory reflex[1]. A subset of T cells in spleen and other tissues express choline acetyltransferase (ChAT), the rate limiting enzyme for the biosynthesis of acetylcholine[1,6, 7]. Here, we characterize these cells further and determine whether ChAT-expressing lymphocytes provide an endogenous cellular mechanism for vasorelaxation in the regulation of blood pressure.

To characterize these ChAT-expressing T cells, we used fluorescence-activated cell sorting (FACS) to isolate splenic ChAT-eGFP$^+$ CD4$^+$ CD44^{high} CD62L^{low} T lymphocytes from transgenic mice expressing enhanced green fluorescence protein (eGFP) under the control of regulatory elements for expression of ChAT[1, 8]. These acetylcholine-producing memory T cells have been demonstrated to control innate immune responses and constitute <10% of the CD4$^+$ CD44^{high} CD62L^{low} population in spleen[1]. Comparison to ChAT-eGFP$^-$ CD4$^+$ CD44^{high} CD62L^{low} T lymphocytes by microarray analysis using Affymetrix Gene 1.0 ST arrays and unsupervised hierarchical clustering of the complete transcriptome showed that ChAT-eGFP$^-$ and ChAT-eGFP$^+$ cells formed distinct clusters (Figure 1a). Transcript expression in ChAT-eGFP$^+$ subsets differed significantly as compared to ChAT-eGFP$^-$ subsets (Figure 1b). Analysis of the significant differences using the Gene Ontology enRIchment anaLysis and visuaLizAtion tool (GOrilla)[9] revealed that genes modulating immune process regulation and negative regulation of leukocyte activation were highly overrepresented (Supplementary Figure 1); and genes modulating G-protein coupled signaling were down-regulated (Supplementary Figure 2). Analysis using the Kyoto Encyclopedia of Genes and Genomes (KEGG) database via the DAVID Bioinformatics tools[10–12] showed over-representation of genes implicated in cytokine-cytokine receptor interaction (Supplementary Table 1). ChAT-eGFP$^+$ T lymphocytes were next analyzed by comparing ChAT expression against 198 different immune cell subsets in the ImmGen dataset[13] (cell types listed in Supplementary Table 2). The ChAT-eGFP$^+$ T cell subset expressed ChAT at significantly higher levels as compared to the other subsets (Figure 1c, Supplementary Table 3). Microarray analysis using unsupervised hierarchical clustering demonstrated that ChAT-eGFP$^+$ T lymphocytes clustered with CD4$^+$ memory and regulatory T lymphocytes (Figure 1c).

ChAT-eGFP$^+$ T cells within the CD4$^+$ CD44^{high} CD62L^{low} T helper cell population defined a unique branch, significantly distinct from other splenic T lymphocyte subsets in hierarchical clustering (Figure 1d). Pairwise Euclidean distance plots of complete gene expression revealed that ChAT-eGFP$^+$ T lymphocytes are highly segregated (Figure 1e). Principal component analysis showed that ChAT-eGFP$^+$ T lymphocytes harbor a T cell gene signature (Supplementary figure 3, Supplementary Table 4), but differ significantly as compared to other T lymphocyte subsets by the first principal component (Figure 1f). Gene ontology classification demonstrated that genes implicated in regulation of leukocyte activation, cytokine receptor activity and G-protein coupled receptor activity were highly over-represented (Supplementary Figures 4–5). Pairwise comparison against 13 other T lymphocyte subsets in the ImmGen database showed that from the cohort of transcription factors implicated in T cell differentiation[14], 41 transcription factors were highly over- or under-represented in the ChAT-eGFP$^+$ T lymphocyte subset (Supplementary Figure 6). We refer to these ChAT$^+$ CD4$^+$ T cells as “CD4 T_{ChAT}.”

We collected tail vein blood from ChAT-eGFP mice and found that ChAT-eGFP$^+$ represented 1.1% of total circulating T lymphocytes (median 95% confidence interval: 0.5%–2%) (Figure 2a). To study whether this relatively small number of lymphocytes modulates blood pressure, we used Cre-lox recombination in mice to selectively ablate ChAT in CD4$^+$ cells. Mice expressing Cre recombinase under the control of the endogenous CD4 promoter (CD4-Cre) were crossed with ChAT-floxed mice to generate CD4$^+$ ChAT

deficient offspring (CD4 ChAT$^{-/-}$). We obtained continuous recordings of carotid blood pressure in awake, freely moving CD4 ChAT$^{-/-}$ and littermate CD4 ChAT$^{+/+}$ mice using telemetry. Both strains displayed normal and similar diurnal blood pressure-variation. Systolic, diastolic, and mean arterial pressures were significantly higher in CD4 ChAT$^{-/-}$ as compared to littermate CD4 ChAT$^{+/+}$ mice (Figure 2b, Supplementary Figure 7–8). Blood pressure recordings as mean arterial tail cuff blood pressure (MAP) in another cohort of CD4 ChAT$^{-/-}$ and CD4 ChAT$^{+/+}$ mice were also significantly higher in CD4 ChAT$^{-/-}$ mice as compared to littermate CD4 ChAT$^{+/+}$ controls (113 ± 3 mmHg, n = 23 vs. 103 ± 4 mmHg, n = 17, p=0.028) (Supplementary Figure 9). Finally, blood pressure measured through an indwelling left carotid artery catheter during anesthesia was also significantly higher in CD4 ChAT$^{-/-}$ as compared to littermate CD4 ChAT$^{+/+}$ mice (Figure 2c). Heart rate was unchanged or decreased in CD4 ChAT$^{-/-}$ mice as compared to CD4 ChAT$^{+/+}$ mice (Supplementary Figure 10, 11). Moreover, echocardiographic assessment of cardiovascular function in these animals revealed that cardiac output, ejection fraction, stroke volume, and fractional shortening of the left ventricle were all significantly decreased in CD4 ChAT$^{-/-}$ as compared to the CD4 ChAT$^{+/+}$ mice (Figure 2d, Supplementary Table 5). Together, these data indicate that deletion of CD4 T_{ChAT} increases vascular resistance and blood pressure in mice.

To study mechanism of lymphocyte-derived acetylcholine in blood pressure regulation, Jurkat T lymphocytes were stably transfected with the pCMV6-mChAT vector engineered to express ChAT. Transfected T lymphocytes (JT_{ChAT}) constitutively produced acetylcholine, whereas non-transfected Jurkat T cells (JT) did not produce detectable levels of acetylcholine (not shown). It has been previously established that acetylcholine mediates vasodilation and hypotension by increasing intracellular Ca^{2+}-levels, and by activating Ser1177 phosphorylation of endothelial nitric oxide synthase (eNOS) to catalyze biosynthesis of NO from L-arginine[15]. To investigate whether JT_{ChAT} stimulates these mechanisms of NO-production here, vascular endothelial cells were pre-loaded with the calcium-responsive Fluo-4 dye and co-incubated with JT_{ChAT}. We observed that co-incubation of JT_{ChAT} cells with endothelial cells triggered a transient increase in endothelial Ca^{2+}-levels as measured by time-lapse fluorescent microscopy, whereas JT failed to increase endothelial intracellular Ca^{2+}-levels (Supplementary Figure 12). Co-incubation of primary ChAT-eGFP^{+} lymphocytes derived from ChAT-eGFP reporter mice or JT_{ChAT} with endothelial cells stimulated Ser1177 phosphorylation; this eNOS phosphorylation was attenuated by atropine (Supplementary Figure 13, 14). Addition of JT_{ChAT} to endothelial cultures also increased production of nitrate and nitrite in the medium, the stable end products of enhanced NO production (Supplementary Figure 15) mediated by exposure of endothelial cells to JT_{ChAT} *in vitro*.

To determine whether JT_{ChAT} mediate vasorelaxation *in vivo*, we measured blood pressure in anesthetized mice following insertion of a catheter (PE10) into the left carotid artery. Infusion of JT_{ChAT} significantly reduced mean arterial pressure within minutes, transiently producing up to a 10% decrease (Figure 3a). In contrast, administration of saline or JT failed to significantly decrease mean arterial pressure from baseline (Figure 3b, 3c). Administration of the muscarinic receptor blocker atropine, or the NOS inhibitor L-N^{G}-Nitroarginine methyl ester (L-NAME) attenuated JT_{ChAT}-mediated decreases in blood

pressure (Figure 3b, 3c, Supplementary Figure 16–17). Administration of JT_{ChAT} failed to significantly reduce mean arterial pressure from baseline in a group of mice with a genetic disruption of eNOS[16] (Supplementary Figure 18), as expected from the prior experiments indicating that JT_{ChAT} enhances endothelial NO production. Together, these results indicate that lymphocyte-derived acetylcholine can decrease blood pressure through a mechanism of endothelium-dependent vasorelaxation.

The identification here of lymphocytes that contribute to blood pressure regulation reveals a previously unknown mechanism in cardiovascular homeostasis. The observation that genetic ablation of ChAT in $CD4^+$ cells results in increased blood pressure in mice indicates that these cells have a homeostatic role in vasorelaxation and regulation of blood pressure. T cells have previously been linked to development of chronic vascular inflammation, atherosclerosis, and chronic increase in blood pressure[17–19]. Putative pathogenic mechanisms of T cells in hypertension, which are incompletely understood, include pro-inflammatory cytokine production, T cell infiltration into vascular walls, and structural changes and stiffening of arterial walls secondary to inflammation[19, 20]. It has also been argued that specific T cell subtypes may play distinct roles in hypertension. For example regulatory T cells may attenuate hypertension by differentially modulating vascular inflammation[21]. Furthermore, it has been suggested that neural signaling originating in the brain stem and circumventricular organs may modulate the role of T lymphocytes in the development of experimental hypertension, and that T cells may play a role in the cerebral regulation of blood pressure[22]. The present findings offer an additional possibility, that a deficiency of CD4 T_{ChAT} could contribute to an increase in blood pressure.

We and others have previously implicated acetylcholine-producing CD4 T_{ChAT} in neural control of inflammation[1, 23, 24]. Blood-borne CD4 T_{ChAT} may deliver acetylcholine to cells devoid of direct cholinergic innervation, including vascular endothelial cells, which respond with NO-dependent vasodilation. Because of the physical constraints within 20–40 μm sized arterioles[25], blood-borne CD4 T_{ChAT} (which are on the order of ~10 μm in diameter) are likely capable of interacting directly with arteriolar endothelial cells, providing a cellular mechanism of acetylcholine-mediated arteriolar relaxation. Prior unexplained evidence of decreased ChAT expression in lymphocytes of hypertensive rats as compared to normotensive rats[26] support a role of blood-borne acetylcholine-producing lymphocytes in vasorelaxation. Our findings that CD4 $ChAT^{-/-}$ mice have an increase in blood pressure render plausible consideration of whether dysregulation of CD4 T_{ChAT} and acetylcholine contributes to the pathogenesis of essential hypertension, and whether this mechanism may underlie hypertension in some cases. This improved understanding of lymphocyte-derived acetylcholine to mediate endothelial-dependent arterial relaxation suggests that it may be possible to enhance cellular acetylcholine release in the vasculature to therapeutically regulate local blood flow and blood pressure, insights that may have implications for developing novel therapy for hypertension.

Moreover, CD4 T_{ChAT} are regulated by neural signals traveling in the vagus and splenic nerves[1]. Ongoing studies of these mechanisms using implanted electrical nerve stimulators[28, 29] may offer another strategy to control the activity of blood pressure-regulating $ChAT^+$ lymphocytes and prevent or reverse hypertension.

Online Methods

Mice

All animal experiments were performed under protocols approved by the Institutional Animal Care and Use Committee of the Feinstein Institute for Medical Research, North Shore-LIJ Health System, the Karolinska Institutet or the University Health Network Animal Care Committee.

Choline acetyltransferase (ChAT)-GFP (B6.Cg-Tg(RP23-268L19-EGFP)2Mik/J), ChAT-floxed (B6.129-Chattm1Jrs/J), and mice expressing Cre recombinase under the control of the endogenous CD4 promoter (CD4-Cre) were purchased from Jackson Laboratories (Bar Harbor, ME, USA). ChAT-floxed and CD4-Cre mice were crossed to generate mice genetically devoid of ChAT in the $CD4^+$ population. Animals were housed at 25°C on a 12-hour light/dark cycle, and acclimatized for at least one week before conducting experiments. Water and regular rodent chow were available *ad libitum*. BALB/c nude (nu/nu) mice 8 to 12 weeks-old were obtained from Taconic. eNOS deficient mice[16] were provided by Drs. Jon Lundberg and Eddie Weitzberg, Karolinska Institutet, Stockholm, Sweden. Cells pooled from ChAT(BAC)-eGFP male and female mice were used for functional and phenotypic characterization. Animals were euthanized using CO_2 asphyxiation or cervical dislocation.

Flow cytometry and cell sorting

ChAT-$eGFP^+$ and ChAT-$eGFP^-$ cells were isolated from spleens of B6.Cg-Tg(RP23-268L19-eGFP)2Mik/J reporter mice by negative selection for $CD4^+$ T cells followed by cell sorting by flow cytometry of the $CD4^+$ $CD44^{hi}$ $CD62L^{low}$ population into $eGFP^+$ and $eGFP^-$ subsets[1]. For cell sorting experiments, an enriched $CD4^+$ T cell suspension was obtained by negative selection ($CD4^+$ T cell isolation kit II, Miltenyi) of spleen cells harvested from male ChAT(BAC)-eGFP mice. The resulting enriched $CD4^+$ cell suspension with >90% purity was then stained with anti-CD44 PE (eBioscience, 12-0441-81), anti-CD4 Pacific Orange (Invitrogen, MCD0430), anti-CD62L PE-Cy7 (eBioscience, 25-0621-82) and anti-CD19 APC (BD Biosciences, BDB550992) antibodies and 7-AAD solution. After gating out $CD19^+$ and gating for $CD62L^{low}$ $CD44^{high}$ cells, a ChAT-$eGFP^-$ and a ChAT-$eGFP^+$ fraction were collected using a FACSAria cell sorter (Becton Dickinson). The resulting fractions were $CD4^+CD44^{high}CD62L^{low}$ChAT-$eGFP^-$ and $CD4^+CD44^{high}CD62L^{low}$ChAT-$eGFP^+$. 100–150,000 cells were sorted into FCS-containing cell culture medium. To improve purity, the freshly sorted cells were immediately sorted again using the same gating strategy, now directly into Trizol solution (Ambion) according to a modified ImmGen protocol (http://www.immgen.org/Protocols) and subsequently frozen at −80° C. Subsequent RNA isolation and Affymetrix Mouse ST 1.0 gene array hybridization experiments were performed by ImmGen[13]. Gene expression of $CD4^+$ ChAT-$eGFP^+$ and $CD4^+$ ChAT-$eGFP^+$ cells were analyzed separately and in the context of subsets of the publicly available ImmGen dataset[13] using the R programming language (see below).

Cell culture

Stable transfection of Jurkat cells—Jurkat cells (originally obtained from ATCC) were a generous gift from Dr. Charles Chu, The Feinstein Institute for Medical Research, Manhasset, NY, U.S.A. pCMV6-mChAT (mChAT ORF in a pCMV6-kan/neo plasmid (ORIGene, Rockville, MD (MC220061)) was nucleofected into Jurkat cells with a mouse T cell kit (Lonza, Allendale, NJ VPA-1006) and a Nucleofector 2b (Lonza). Transformed cells were selected over 2 weeks with G418 (400 mg/mL) in RPMI containing 10% FBS. Isolated cells were individually selected by pipet and serial dilution for monoclonal populations, then grown for an additional month to ensure stable chromosomal integration. Monoclonal lines were analyzed for ChAT expression by Western blotting. Jurkat cell lines tested negative for Mycoplasma sp., EBV, HAdV, Hantaan, HCMV, Hepatitis A, Hepatitis B, Hepatitis C, HHV 6, HHV 8, HIV1, HIV2, HSV 1, HSV 2, HTLV 1, HTLV 2, LCMV, Seoul, Sin Nombre, VZV.

Co-incubation experiments—Primary $ChAT^+$ lymphocytes or Jurkat T lymphocytes (JT) or pCMV6-mChAT-transfected JT (JT_{ChAT}) were co-incubated with either human endothelial cells derived from pulmonary microcirculation or murine endothelial cells[30, 31]. Human PEC1.6ST cells were seeded in 6-well plates in Endothelial Cell Growth Medium MV with supplement mix C-39225 (PromoCell) and experiments were performed at confluency. 2 x 10^6 $ChAT^+$ Jurkat T cells, 2 x 10^6 Jurkat T cells, 10^6 primary $ChAT^+$ lymphocytes or acetycholine to a concentration of 100 uM in fresh medium was added to the endothelial cell culture, and cells incubated for one hour. During co-culture experiments, cells were kept in a modular incubator chamber (Billups-Rothenberg, Del Mar, CA, USA) in a microenvironment within the chamber of 37 °C, 1% O_2, 5% CO_2 and 100% humidity[32]. Culture wells were subsequently washed twice with cold PBS and removal of non-adherent cells verified by microscopy. Protein was extracted using T-PER solution (Thermo Scientific) in the presence of HALT protease and phosphatase inhibitors (Thermo Scientific) according to manufacturer instructions, and lysates stored at −80 C until analysis using Western blot. Membranes were probed with anti-peNOS (Cell Signaling) and anti-beta actin (GeneScript) and developed with standard reagents (Pierce). Images were acquired on a GS-800 calibrated densitometer (Bio-Rad) and images analyzed using Image Studio software (Licor). Nitrite and nitrate in supernatants was measured using the Nitrate/Nitrite Colorimetric Assay Kit (Cayman Chemical, Ann Arbor, MI) according to manufacturer instructions.

Murine lung microvascular endothelial cells were isolated and cultured as previously described[31]. In brief, fresh mouse lungs were rinsed, minced aseptically into small pieces and digested in collagenase A (1 mg/mL, Worthington, NJ) at 37°C for 60 minutes with occasional agitation. The single cell suspension was filtered through sterile 40 μm cell strainer, washed in DMEM medium containing 10% fetal calf serum (10% FCS-DMEM), and incubated with magnetic beads conjugated with anti-mouse CD31 antibody (Invitrogen, Carlsbad, CA) at 4°C for 30 minutes. The bead-bound cells were recovered by placing the tube in a magnetic separation rack, washed with 10% FCS-DMEM, collected and cultured in DMEM medium containing 10% FCS, 2 mM l- glutamine, 2 mM sodium pyruvate, 20 mM Hepes, 1% nonessential amino acids, 100 μg/mL streptomycin, 100 U/mL penicillin, 100

μg/mL heparin, and 100 μg/mL EC growth supplement. EC phenotype was confirmed by positive staining of multiple endothelial-specific markers.

Calcium measurements—Endothelial cells derived from pulmonary microvasculature[31] were seeded onto glass coverslips 16–24 hours prior to use in calcium imaging experiments. The coverslips were placed in a stainless steel imaging cell chamber (Attofluor Cell Chamber, Life Technologies, Grand Island, New York, USA). Within this chamber, the cells were washed with DMEM and loaded with the calcium-sensitive Fluo-4 NW in DMEM with probenecid (Fluo-4 NW Calcium Assay Kit, Molecular Probes, Eugene Oregon, USA) for 45–60 min at 37 °C under 5% CO2. The imaging chamber was placed in a temperature-controlled Leiden chamber holder mounted on the stage of an Axiovert 200M inverted fluorescence microscope (Carl Zeiss Microscopy, Thornwood, New York, USA) equipped with a 40X, 0.60 numerical aperture objective. Data were recorded every 10 seconds by illuminating the sample with light from a mercury lamp passing through an excitation filter (470 nm ± 40) before being directed at the cells via a 495 nm dichroic mirror. A single field visualized in each experiment. Emitted light was captured by a cooled CCD camera (AxioCam monochromatic, Carl Zeiss Microscopy, Thornwood, New York, USA) following passage through a 525 nm ± 50 emission filter. The image acquisition setup was controlled by Axiovision 4.7 software (Carl Zeiss Microscopy, Thornwood, New York, USA).

After being placed on the microscope stage, cells were washed once with HEPES-buffered and indicator-free DMEM containing acetylcholine esterase inhibitor. Baseline fluorescence was recorded for 2 min at which time cells were treated with 0.1 mM acetylcholine or co-culture with 10^6/mL of Jurkat T lymphocytes, pCMV6-mChAT vector-transfected Jurkat T lymphocytes, primary $ChAT^+$ lymphocytes, or primary $ChAT^-$ lymphocytes. Intracellular fluorescence was monitored for an additional 5 minutes before concluding the experiment by treatment with 10 μM ionomycin (Sigma-Aldrich, St-Louis, MO, USA).

The acquired images were exported to ImageJ software for analysis. The mean fluorescence intensity values of 6–31 cells per experiment were extracted for each time point and normalized to the average baseline intensity. Individual cell data was then averaged for each experiment. To quantify the treatment response, the average fluorescence in the one-minute intervals immediately before and after treatment was calculated.

Blood pressure measurement

Arterial catheterization—Adult C57Bl/6 male mice (23–30 g) were anaesthetized using isoflurane and maintained on a heating pad at rectal temperature 37.5–38 °C throughout the experiment. An incision on the left side of the neck followed by blunt dissection was performed to gain access to the carotid artery. The artery was tied off towards the head before cannulation. A PE 10 catheter (0.28 mm inner diameter and 0.61 mm outer diameter) was inserted in the artery and secured with USP 6.0 silk suture. Arterial blood pressure was then monitored via the saline filled catheter with recording system (AD-instruments). Cells for infusion were spun down and resuspended in NaCl prior to experiments. The suspensions (200 uL) were pre-warmed and administered via a T-branch on the catheter. In all experiments, the animals were allowed to stabilize for 5 min after catheter insertion and after

that an initial record of blood pressure with saline injection was recorded followed by an initial 10 s-3 min baseline recording. Animals with hypotension were excluded. The infusion was administered subsequently during approximately ten seconds, and blood pressure recorded every 10 s for ≥9 min. Blood pressure change over time was assessed by calculating the area under the curve for the baseline normalized MAP tracing of cells and then calculating the area under the curve (as exemplified by the shaded areas in Figure 4b) between the 240^{th} and the 780^{th} second and/or analyzed using 2-way ANOVA followed by Bonferroni post-hoc test using GraphPad Prism. The baseline was calculated as the mean MAP over 3 minutes before injection. Jurkat T lymphocytes (JT) or $ChAT^{hi}$ lymphocytes (JT_{ChAT}) (50×10^7 cells in 200 uL saline or the number of cells indicated in the figures) were administered, with or without pretreatment with atropine (0.05 mg/kg) or L-NAME (10 mg/kg). The cells were injected 30 and 10 min after Atropine and L-NAME respectively. In experiments with eNOS deficient mice, approx. 1 year of age, saline, JT or JT_{ChAT} were infused sequentially after a ≈10 s base line and blood pressure monitored for approx. 4 minutes after each infusion. Animals with recordings interrupted before 4 min. were excluded. In anesthesized CD4-$Cre^{+/0}$ x $ChAT^{flox/flox}$ mice and their littermate controls, a 1.2 F pressure catheter (Transonic, US) in the right carotid artery was used for measurements and data acquired using Biopack 3.8 software.

Telemetry hemodynamic recording—12 week old mice were anesthetized using 2% isoflurane oxygen mixture and placed on a heating pad. A midline incision was made on the neck and the right common carotid was isolated. The flexible tip of a hemodynamic telemetry unit (Data Sciences International, PA-C10) was introduced into the carotid after puncturing the carotid with a 26 gauge needle. The catheter was secured in place using a 6-0 silk suture. The body of the telemetry unit was placed sub-dermally close to the abdomen. After 5 days of recovery, arterial pressures were recorded for 10 seconds every 1 minute over a 48 hour period. Data analysis and acquisition was performed using DataQuest A.R.T software (Data Sciences International). The investigator was blinded for animal group at time of unit implantation and for the analysis.

Echocardiography—Mice were anesthetized using 1.5% isoflurane oxygen mixture. Mice were placed on a heating pad and body temperature was maintained between 37.3 to 37.6 °C for the duration of the measurements. The investigator was fully blinded for animal group for examination and analysis. Transthoracic M-mode echocardiographic examination was performed from the long axis view of the heart at the level of the postermedial papillary muscle using a Vevo 7700 system (VisualSonics) with a 30 MHz ultrasonic linear transducer scanning head. The papillary muscles were not included in the measurements. Measurements of left ventricle diastolic diameter (LVDd) and left ventricle systolic diameter (LVDs) were done under Time Motion-mode (TM-Mode) and were averaged from at least 3 cardiac cycles. End Systolic volume (ESV) and end diastolic volumes (EDV) were calculated using Vevo770 heart analysis package (volume estimate based on Teichholz's formula). SV was calculated as EDV-ESV; cardiac output (CO) as SV x heart rate (HR); ejection fraction (EF) as (EDV-ESV)/EDV x 100; and fraction shortening (FS) was calculated as (LVDd-LVDs)/LVDd x 100.

Non-invasive blood pressure measurement—Non-invasive blood pressure measurements were conducted in male CD4-Cre$^{+/0}$ x ChAT$^{flox/flox}$ mice and their littermate controls at 7 weeks of age using the CODA NIBP tail-cuff device (Kent Scientific Corp., Torrington, CT, USA) as per the manufacturer's instructions. Mice were anesthestized using isoflurane (4–5% induction, 1.5% maintenance) and the NIBP and heart rate recorded every 45 seconds for 10–12 minutes. The serial measurements were then averaged. All measurements were conducted during the animals' light cycle.

Statistical analysis

Gene expression—RNA isolation and Affymetrix Mouse ST 1.0 gene array hybridization was performed by ImmGen (http://www.immgen.org/Protocols). Samples with high and comparable array expression levels of CD3, CD4, and CD44 were included in the analysis.

Data analysis was performed using the R programming language. The raw datasets from ImmGen[13] (Release September 2012) were downloaded from NCB's GEO data repository (GSE15907). After removal of control, test and certain variant subsets (Supplementary Table 2) this dataset comprises 2–7 replicates of 198 different immune cell subsets.

The R/Bioconductor package "oligo" was used for data import and normalization (through 'rma') and the packages "pd.mogene.1.0.st.v1", "mogene10sttranscriptcluster.db", and the getNetAffx function from the "oligo" package for annotation of transcripts. This annotation process created a set of 476 transcripts that were identical to the 9th decimal, which were removed. See also Ericson J *et al* "ImmGen microarray gene expression data: Data Generation and Quality Control pipeline", available at http://www.immgen.org/. We furthermore removed transcripts without any annotated gene symbol available, and proceeded to analyze the remaining dataset of 24925 unique transcripts IDs.

Expression data from ChAT-eGFP^{+} and ChAT-eGFP^{-} subsets were merged with the ImmGen data using a ratio-based method for batch effect removal[33]. To accomplish this, overlapping groups between batches were used as reference samples. The ImmGen dataset contains CD4^{+} CD44^{high} CD62L^{low} Memory T cells from the spleen, labeled T. 4Mem44h62l.Sp. According to available data on ChAT-eGFP^{+} and ChAT-eGFP^{-} T cell populations[1], >90% of this subset consists of CD4^{+} CD44^{high} CD62L^{low} ChAT-eGFP^{-} lymphocytes, and we therefore used the T.4Mem44h62l.Sp and CD4^{+} CD44^{high} CD62L^{low} ChAT-eGFP^{-} T cell subsets to normalize expression data between ImmGen and ChAT_eGFP reporter samples. Each batch was first normalized separately using 'rma'. Then, each sample was divided by the mean of the T.4Mem44h62l.Sp or CD4^{+} CD44^{high} CD62L^{low} ChAT-eGFP^{-} subsets, respectively. Data were subsequently merged into a ratio matrix for transcript IDs.

Hierarchical clustering analysis was performed using complete linkage clustering with a Euclidean distance measure. Differential analysis in group comparisons was performed using the R/Bioconductor package "limma"[34]. The David Bioinformatics Annotation Tool (http://david.abcc.ncifcrf.gov/)[10, 11] was utilized for Gene Ontology (GO) and KEGG pathway enrichment analysis. The Gene Ontology enRIchment anaLysis and visuaLizAtion tool (GOrilla)[9, 35] was used for further analysis and visualization of GO terms.

In the analysis of transcription factor expression across the dataset, the absolute value of the log-transformed expression values of each transcription factor in 14 splenic T cell samples was calculated. Since expression data are in ratio format this presents a symmetry for high and low expression values. The absolute values of the log-transformed expression ratios were then ranked for each transcription factor across the 14 samples. For transcription factors that were ranked highest in the ChAT_eGFP^{+} T cell sample, pairwise comparisons for differential expression between the ChAT_eGFP^{+} T cell sample and each of the other 13 splenic T cell subsets were performed. Transcription factors for which ChAT_eGFP+ samples were ranked highest and significantly different in each pairwise comparison were plotted in a heat map (FDR-adjusted $P<0.05$ in any pairwise comparison between ChAT_eGFP+ T and the other T cells samples).

Sample size was chosen depending on available data (Immgen) and for experiements according to prior experience with similar experiments in the involved research laboratories. Differences between experimental groups were analyzed using one-way ANOVA followed by Dunnet's or Bonferoni post-hoc analysis or Student's *t* test as indicated. Blood pressure data obtained using telemetry was analyzed using repeated measures ANOVA. $P < 0.05$ was considered significant.

Code Availability—The specific R computer code used to generate the bioinformatics data will be made available upon request.

Supplementary Material

Refer to Web version on PubMed Central for supplementary material.

Acknowledgments

We thank the flow cytometry facility at the Feinstein Institute, the laboratory of Christophe Benoist at Harvard Medical School for assistance, and Prof. Göran K. Hansson for comments. This work was supported by the following grants: NIH, NIGMS RO1 GM57226 to KJT, NIGMS RO1 GM098446 to HY and NIGMS RO1GM089807 to KJT and VAP, VR 2013-3003 to AA, NIAID R01 029690 to TLR, and Knut and Alice Wallenberg's Foundation 2014.0212, The Swedish Heart-Lung Foundation 20150767 and Svenska Läkaresällskapet to PSO.

References

1. Rosas-Ballina M, et al. Acetylcholine-synthesizing T cells relay neural signals in a vagus nerve circuit. Science (New York, N Y). 2011; 334:98–101.
2. SEVENTY-FOURTH ANNUAL MEETING OF THE British Medical Association. BMJ (Clinical research ed). 1906; 2:1760–1816.
3. Furchgott RF, Zawadzki JV. The obligatory role of endothelial cells in the relaxation of arterial smooth muscle by acetylcholine. Nature. 1980; 288:373–376. [PubMed: 6253831]
4. Fleming I, Busse R. NO: the primary EDRF. J Mol Cell Cardiol. 1999; 31:5–14. [PubMed: 10072711]
5. Mulvany MJ, Aalkjaer C. Structure and function of small arteries. Physiol Rev. 1990; 70:921–961. [PubMed: 2217559]
6. Andersson U, Tracey KJ. Reflex principles of immunological homeostasis. Annual review of immunology. 2012; 30:313–335.

7. Olofsson PS, et al. alpha7 Nicotinic Acetylcholine Receptor (alpha7nAChR) Expression in Bone Marrow-Derived Non-T Cells Is Required for the Inflammatory Reflex. Molecular medicine. 2012; 18:539–543. [PubMed: 22183893]
8. Tallini YN, et al. BAC transgenic mice express enhanced green fluorescent protein in central and peripheral cholinergic neurons. Physiol Genomics. 2006; 27:391–397. [PubMed: 16940431]
9. Eden E, Navon R, Steinfeld I, Lipson D, Yakhini Z. GOrilla: a tool for discovery and visualization of enriched GO terms in ranked gene lists. BMC bioinformatics. 2009; 10:48. [PubMed: 19192299]
10. Huang da W, Sherman BT, Lempicki RA. Systematic and integrative analysis of large gene lists using DAVID bioinformatics resources. Nature protocols. 2009; 4:44–57. [PubMed: 19131956]
11. Huang da W, Sherman BT, Lempicki RA. Bioinformatics enrichment tools: paths toward the comprehensive functional analysis of large gene lists. Nucleic acids research. 2009; 37:1–13. [PubMed: 19033363]
12. Kanehisa M, Goto S, Sato Y, Furumichi M, Tanabe M. KEGG for integration and interpretation of large-scale molecular data sets. Nucleic acids research. 2012; 40:D109–114. [PubMed: 22080510]
13. Heng TS, Painter MW. Immunological Genome Project C. The Immunological Genome Project: networks of gene expression in immune cells. Nature immunology. 2008; 9:1091–1094. [PubMed: 18800157]
14. Mingueneau M, et al. The transcriptional landscape of alphabeta T cell differentiation. Nature immunology. 2013; 14:619–632. [PubMed: 23644507]
15. Dimmeler S, et al. Activation of nitric oxide synthase in endothelial cells by Akt-dependent phosphorylation. Nature. 1999; 399:601–605. [PubMed: 10376603]
16. Huang PL, et al. Hypertension in mice lacking the gene for endothelial nitric oxide synthase. Nature. 1995; 377:239–242. [PubMed: 7545787]
17. Laurat E, et al. In vivo downregulation of T helper cell 1 immune responses reduces atherogenesis in apolipoprotein E-knockout mice. Circulation. 2001; 104:197–202. [PubMed: 11447086]
18. Robertson AK, et al. Disruption of TGF-beta signaling in T cells accelerates atherosclerosis. The Journal of clinical investigation. 2003; 112:1342–1350. [PubMed: 14568988]
19. Guzik TJ, et al. Role of the T cell in the genesis of angiotensin II induced hypertension and vascular dysfunction. The Journal of experimental medicine. 2007; 204:2449–2460. [PubMed: 17875676]
20. Harrison DG, et al. Inflammation, immunity, and hypertension. Hypertension. 2011; 57:132–140. [PubMed: 21149826]
21. Matrougui K, et al. Natural regulatory T cells control coronary arteriolar endothelial dysfunction in hypertensive mice. The American journal of pathology. 2011; 178:434–441. [PubMed: 21224080]
22. Marvar PJ, Harrison DG. Stress-dependent hypertension and the role of T lymphocytes. Exp Physiol. 2012; 97:1161–1167. [PubMed: 22941978]
23. Olofsson PS, Rosas-Ballina M, Levine YA, Tracey KJ. Rethinking inflammation: Neural circuits in the regulation of immunity. Immunological reviews. 2012; 248:188–204. [PubMed: 22725962]
24. Kawashima K, Fujii T, Moriwaki Y, Misawa H, Horiguchi K. Reconciling neuronally and nonneuronally derived acetylcholine in the regulation of immune function. Annals of the New York Academy of Sciences. 2012; 1261:7–17. [PubMed: 22823388]
25. Bearden SE, Payne GW, Chisty A, Segal SS. Arteriolar network architecture and vasomotor function with ageing in mouse gluteus maximus muscle. J Physiol. 2004; 561:535–545. [PubMed: 15388783]
26. Fujimoto K, Matsui M, Fujii T, Kawashima K. Decreased acetylcholine content and choline acetyltransferase mRNA expression in circulating mononuclear leukocytes and lymphoid organs of the spontaneously hypertensive rat. Life sciences. 2001; 69:1629–1638. [PubMed: 11589503]
27. Lataro RM, Silva CA, Tefe-Silva C, Prado CM, Salgado HC. Acetylcholinesterase Inhibition Attenuates the Development of Hypertension and Inflammation in Spontaneously Hypertensive Rats. Am J Hypertens. 2015
28. Tracey KJ. Shock Medicine. Scientific American. 2015; 312:28–35.
29. Birmingham K, et al. Bioelectronic medicines: a research roadmap. Nature reviews. 2014; 13:399–400.

30. Krump-Konvalinkova V, et al. Generation of human pulmonary microvascular endothelial cell lines. Laboratory investigation; a journal of technical methods and pathology. 2001; 81:1717–1727. [PubMed: 11742042]

31. Ye X, Ding J, Zhou X, Chen G, Liu SF. Divergent roles of endothelial NF-kappaB in multiple organ injury and bacterial clearance in mouse models of sepsis. The Journal of experimental medicine. 2008; 205:1303–1315. [PubMed: 18474628]

32. Ahmed MN, et al. Extracellular superoxide dismutase overexpression can reverse the course of hypoxia-induced pulmonary hypertension. Molecular medicine (Cambridge, Mass. 2012; 18:38–46.

33. Luo J, et al. A comparison of batch effect removal methods for enhancement of prediction performance using MAQC-II microarray gene expression data. The pharmacogenomics journal. 2010; 10:278–291. [PubMed: 20676067]

34. Smyth, GK. Bioinformatics and Computational Biology Solutions using R and Bioconductor. Gentleman, R.Carey, V.Dudoit, S.Irizarry, R., Huber, W., editors. Springer; New York: 2005. p. 397-420.

35. Eden E, Lipson D, Yogev S, Yakhini Z. Discovering motifs in ranked lists of DNA sequences. PLoS computational biology. 2007; 3:e39. [PubMed: 17381235]

Figure 1a

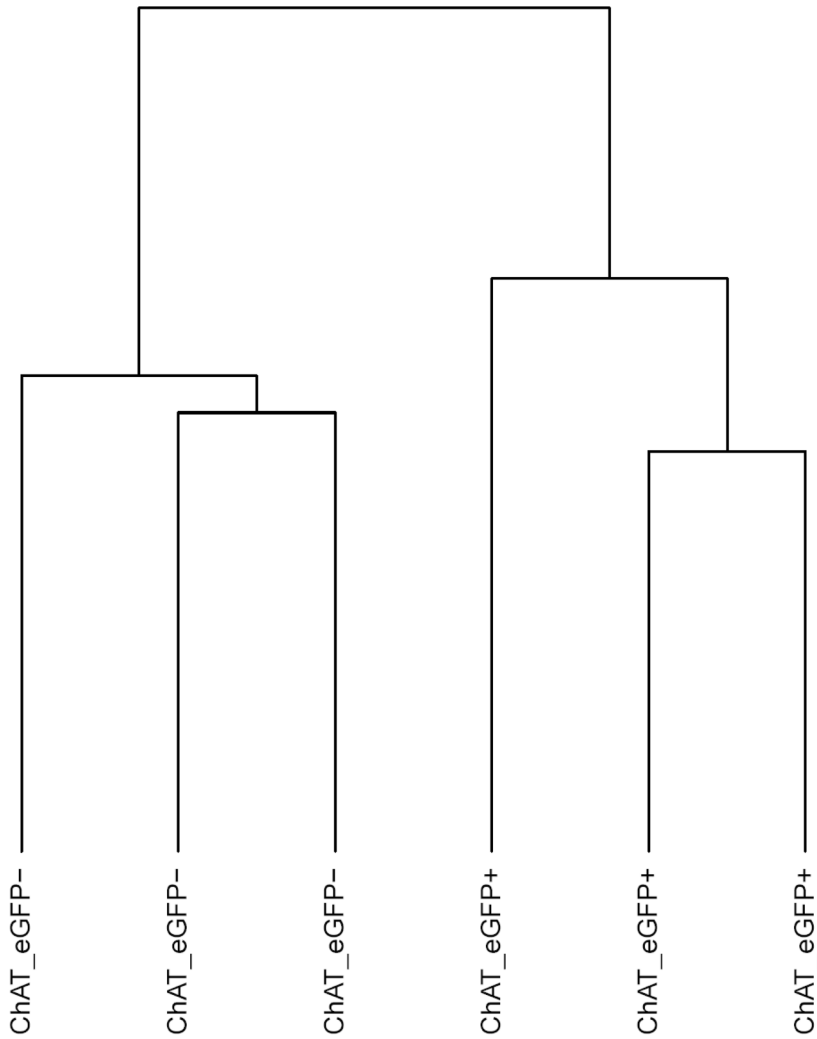

Figure 1b

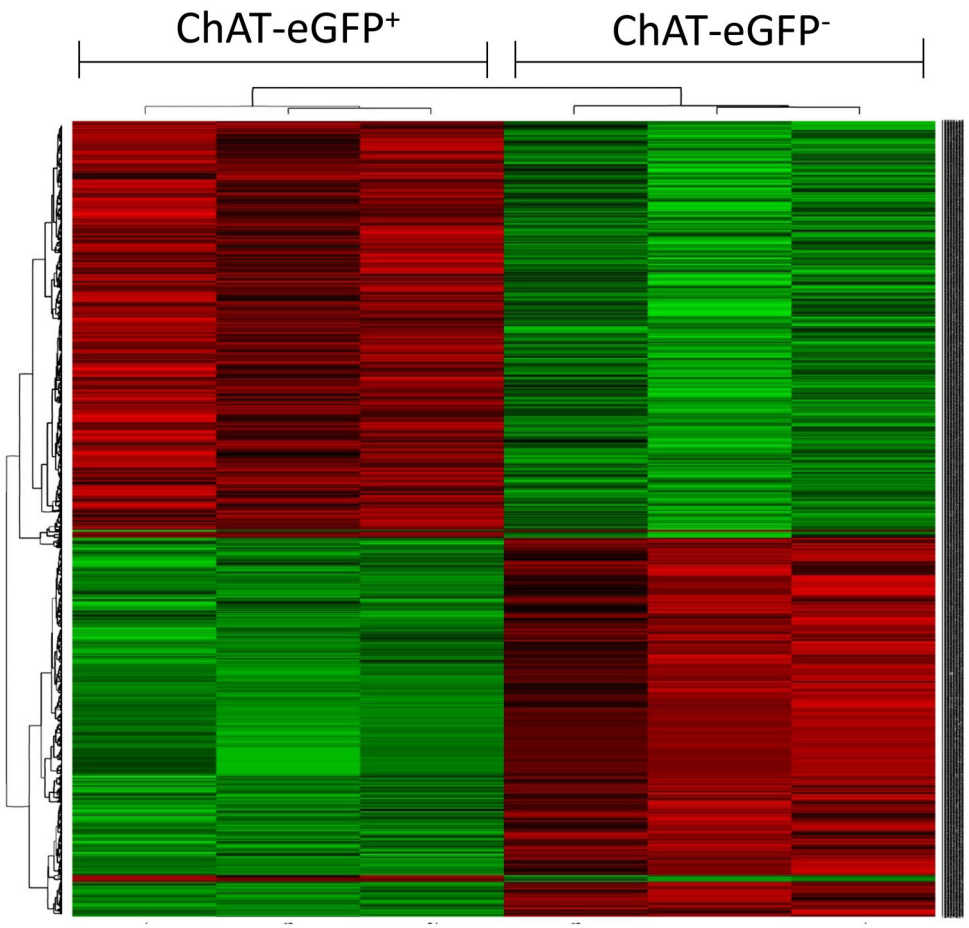

Figure 1c

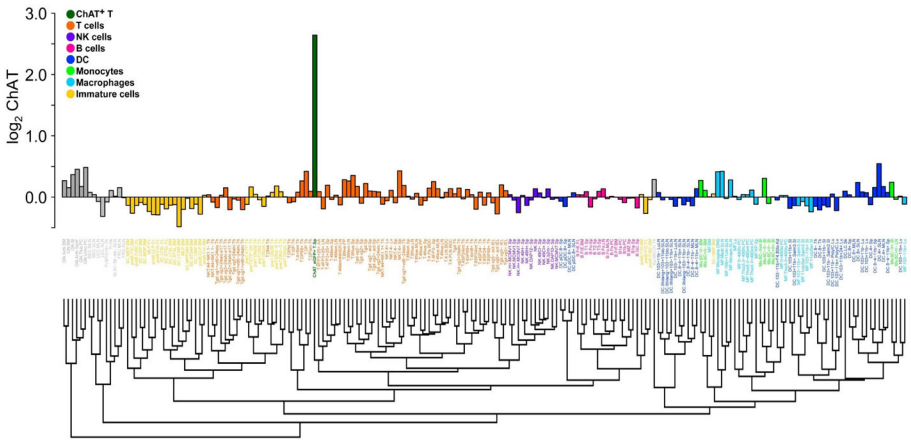

Figure 1d

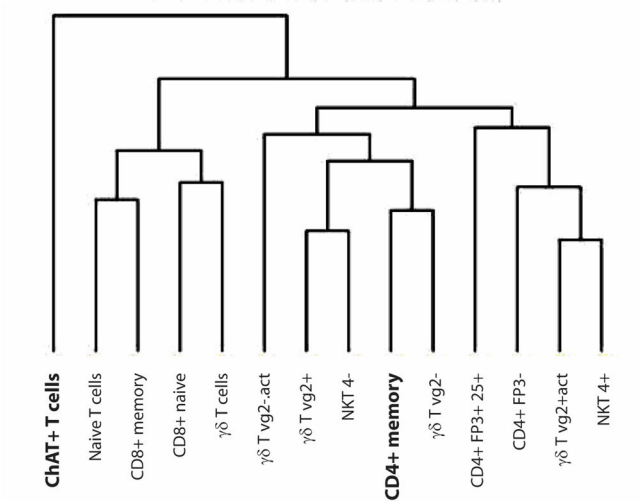

Figure 1e

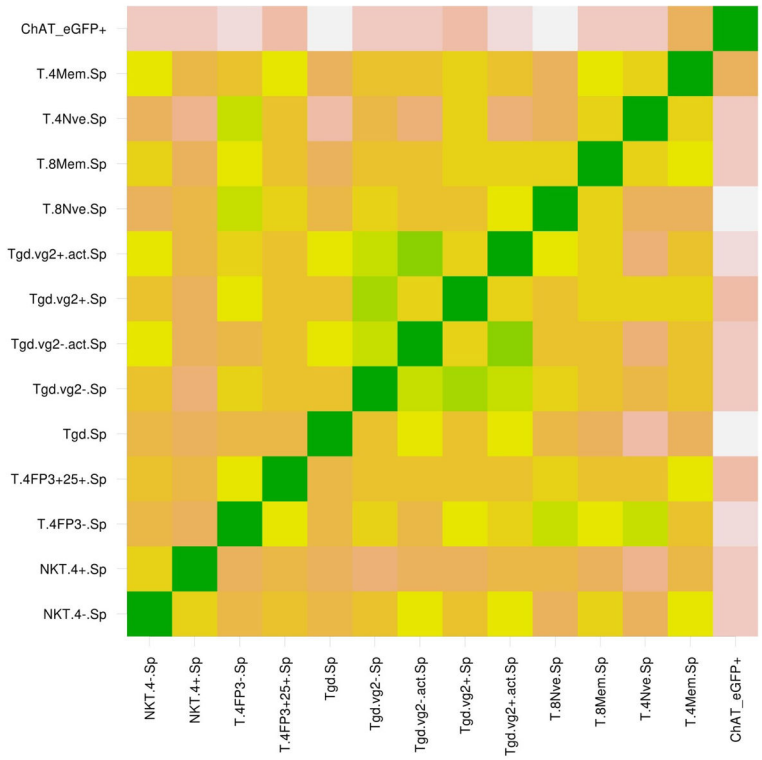

Figure 1f

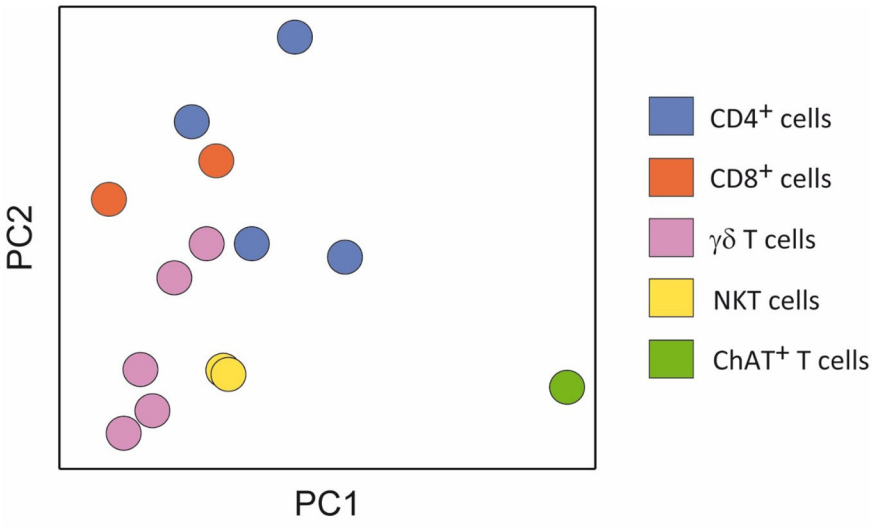

Figure 1. Gene expression analysis reveals differences between CD4^{+} CD44^{hi} CD62L^{low} ChAT-eGFP^{+} and ChAT-eGFP^{-} T cells

a) RNA from the ChAT-eGFP^{+} and ChAT-eGFP^{-} subsets of CD4^{+} CD44^{hi} CD62L^{low} T cells was analyzed by Affymetrix Gene ST 1.0 arrays. Unsupervised hierarchical clustering of the whole transcriptome of six samples, each from ≥3 pooled murine spleens, is shown. b) The 1288 transcripts with significantly different expression between the subsets ($P<0.05$ with Benjamini Hochberg correction) were studied using unsupervised hierarchical clustering and plotted in a heat map. 1281 out of 1288 transcripts had a fold change of >1.5 (n=3). c) Bottom: Unsupervised global hierarchical clustering of gene expression in ChAT-eGFP^{+} T lymphocytes and 198 other immune cell subsets from the ImmGen dataset. Top: Expression level of ChAT across the 199 different immune cell subsets. Bar color indicates cell type as shown in the figure insert. | Gene expression in CD4^{+} CD44^{hi} CD62L^{low} ChAT-eGFP^{+} T cells was analyzed in the context of 13 other subsets isolated from spleen in the ImmGen dataset. d) Unsupervised hierarchical clustering of gene expression in the T cell subsets derived from spleen. e) Heat map of pair-wise Euclidian distances and f) principal component analysis of gene expression in the splenic T cell subsets.

Figure 2a

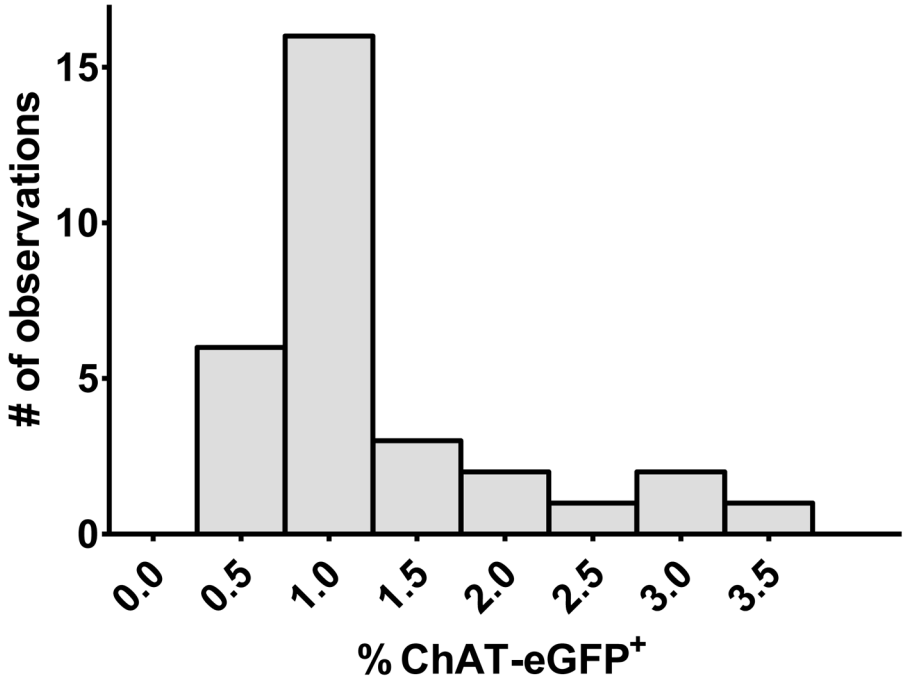

Figure 2b

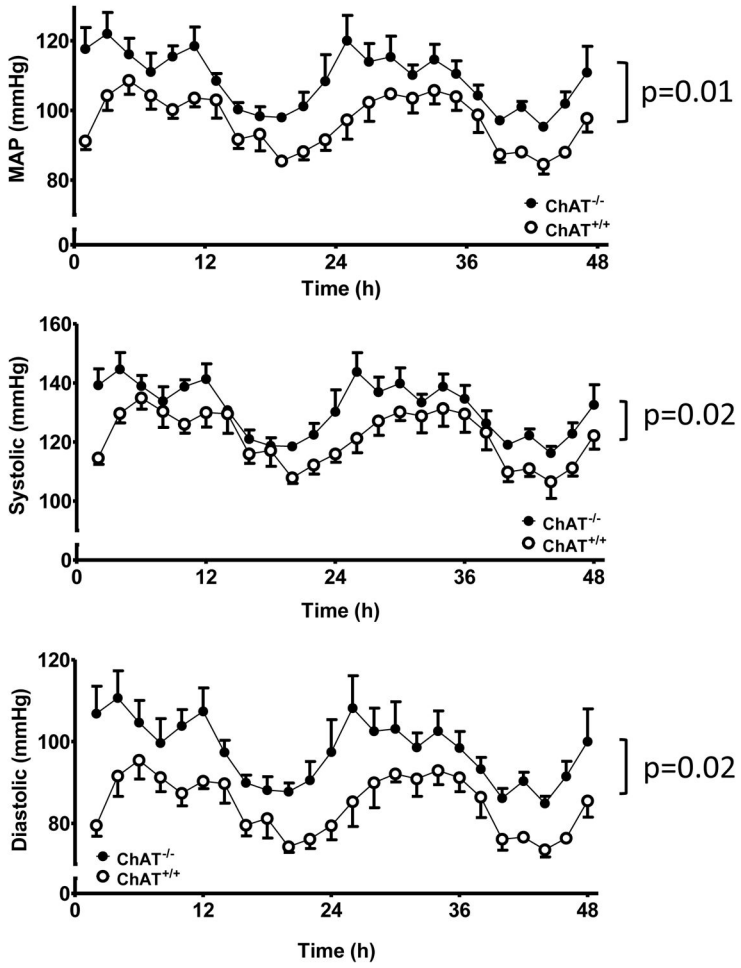

Figure 2c

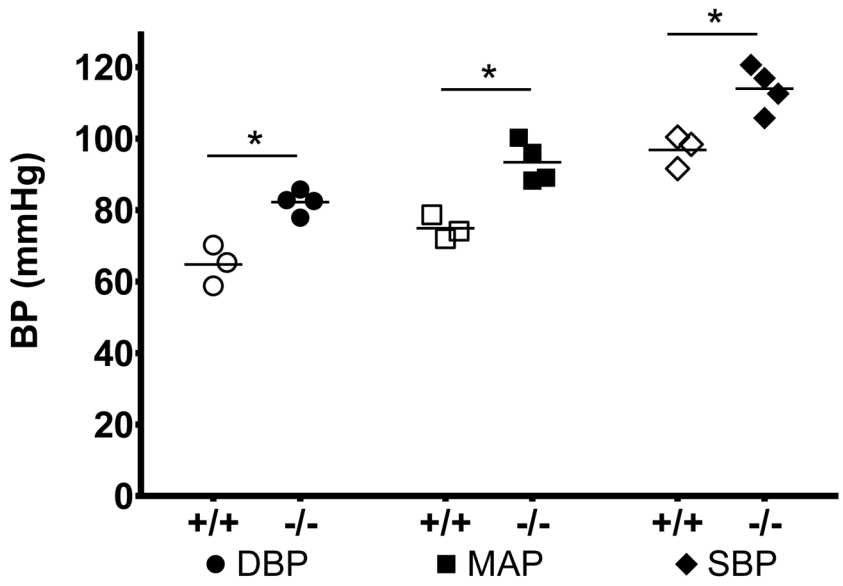

Figure 2d

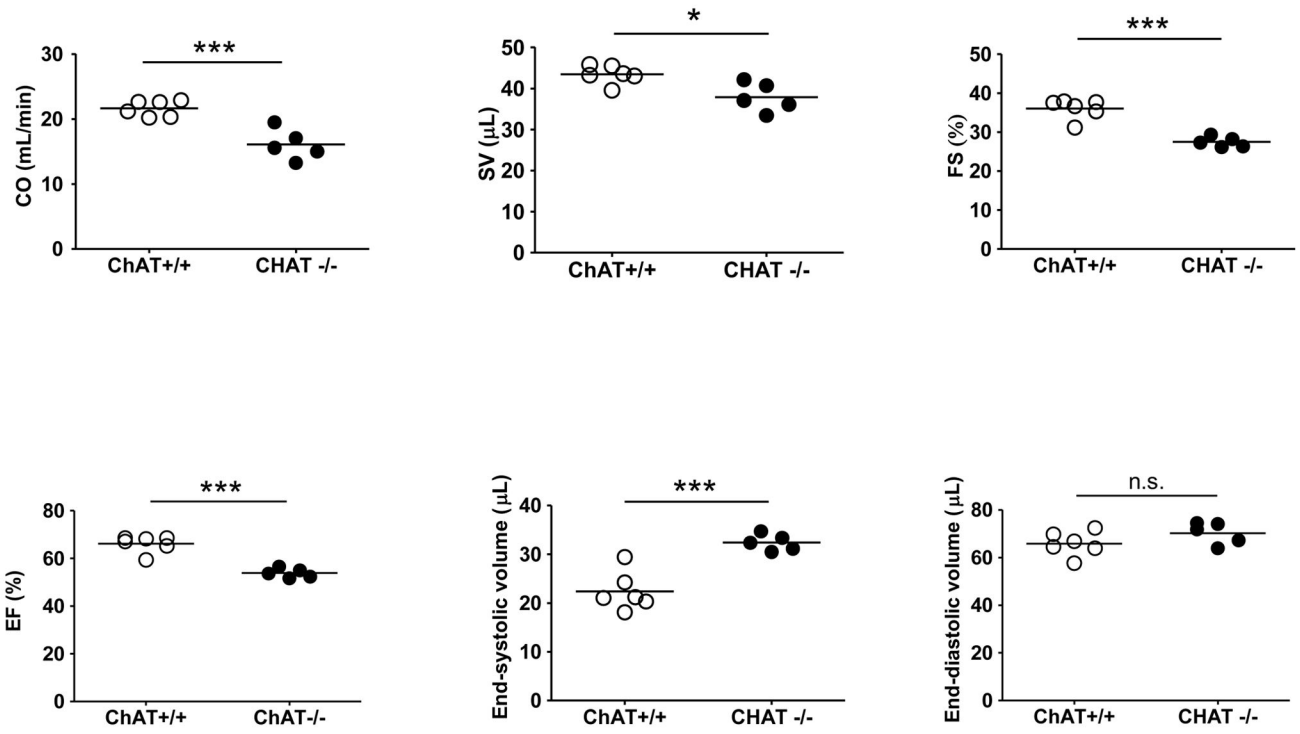

Figure 2. Increased blood pressure in mice with genetic ablation of choline acetyltransferase^{+} CD4^{+} cells

a) Blood from ChAT-eGFP reporter mice 6–12 weeks of age obtained by tail bleed was analyzed by flow cytometry to determine the fraction of ChAT-eGFP^{+} cells of CD3^{+} cells in each mouse. A histogram of the compiled data is plotted. b) Blood pressure measured by telemetry over 48 h in awake 12 weeks old ChAT-deficient CD4-Cre$^{0/+}$ x ChAT$^{loxP/loxP}$ (ChAT$^{-/-}$, n=6) and their CD4-Cre$^{0/0}$ x ChAT$^{loxP/loxP}$ (ChAT$^{+/+}$, n=4) littermate controls. Data were analyzed using repeated measures ANOVA. c) Blood pressure (BP) as measured by an indwelling catheter in the left carotid artery in anesthetized ChAT$^{+/+}$ (+/+, n=3) and ChAT$^{-/-}$ (−/−, n=4) mice. D – diastolic, M – mean arterial, S – systolic. * - P < 0.05 (two-tailed Student's *t* test). d) Echocardiographic measurements in 10–11 weeks old ChAT$^{+/+}$ (n=6) and ChAT$^{-/-}$ (n=5) mice. CO – cardiac output, SV – stroke volume, FS – fractional shortening, EF – ejection fraction. * - P < 0.05 (two-tailed Student's *t* test).

Figure 3a

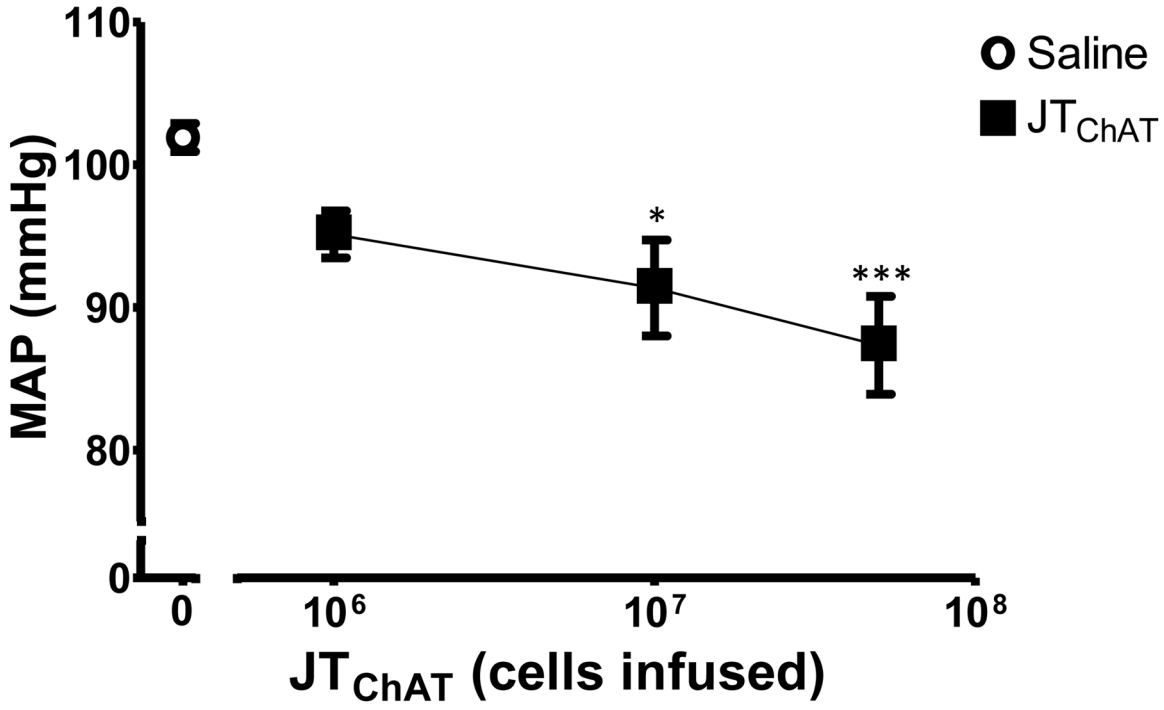

Figure 3b

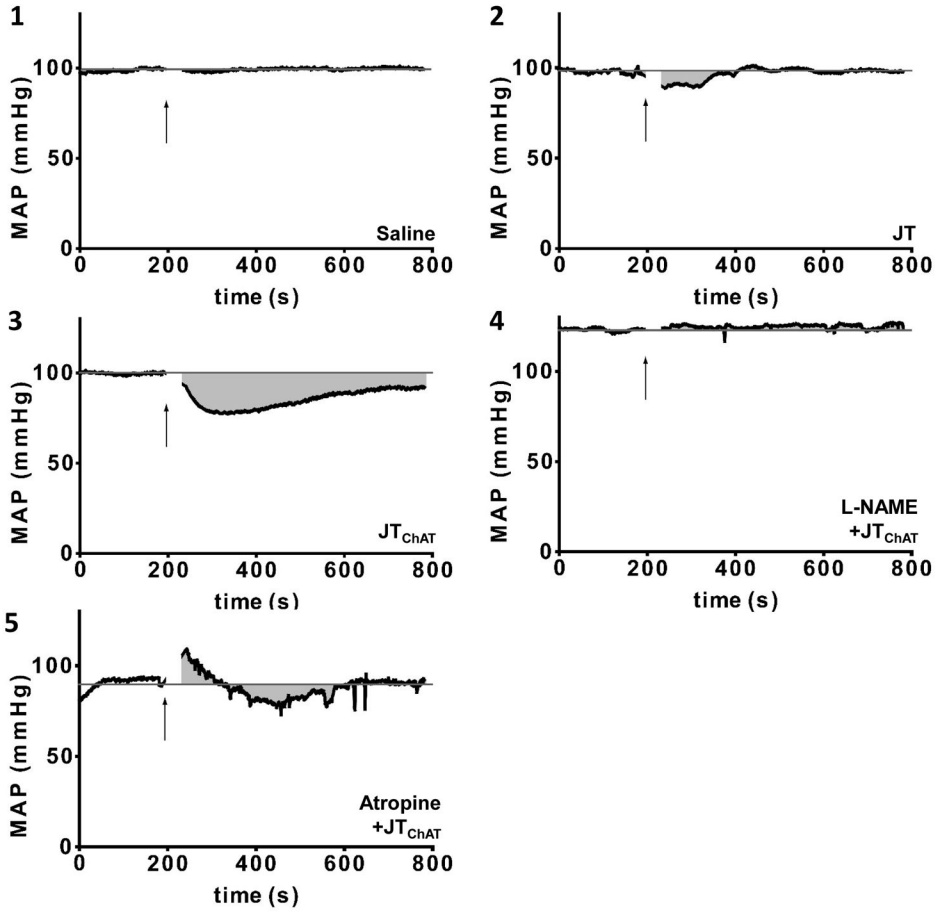

Figure 3c

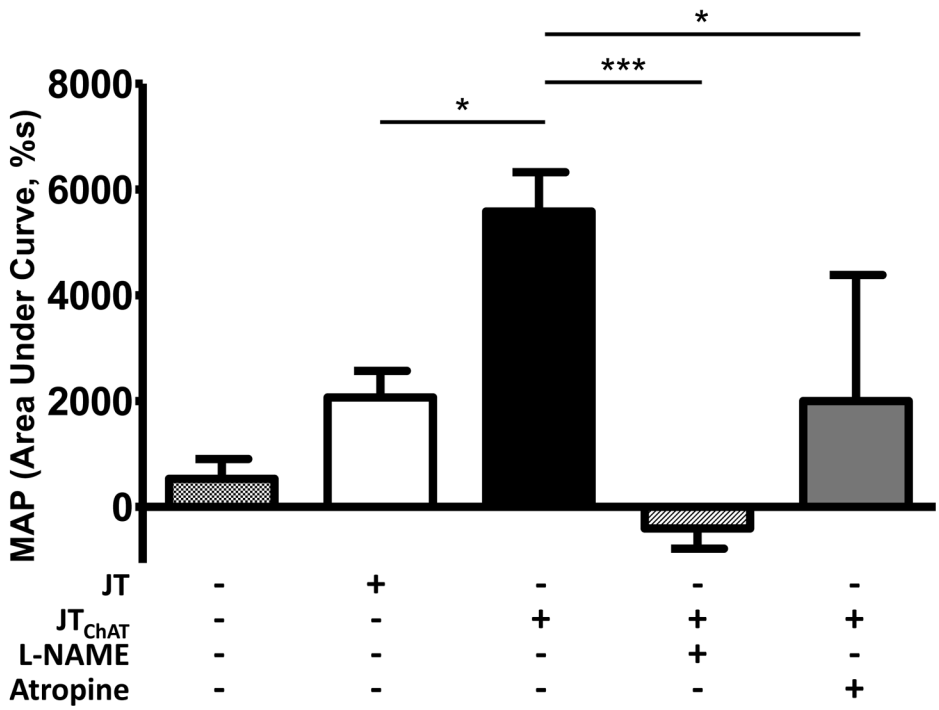

Figure 3. Infusion of JT_{ChAT} lymphocytes lowers blood pressure

a–c) Mean arterial blood pressure was measured by a catheter inserted in the left carotid artery in anesthetized wild-type C57Bl/6 mice. a) Mean MAP over ~9 min. after infusion of JT_{ChAT} lymphocytes or saline. Open circle – saline (n=14). Closed squares - JT_{ChAT} (n=7–13). * - $p<0.05$, *** - $p<0.001$ JT_{ChAT} vs Saline by ANOVA followed by Bonferroni post-hoc test. b) Tracings of mean arterial pressure (MAP) over time in mice infused with (1) saline, (2) JT lymphocytes, or (3) JT_{ChAT} lymphocytes, or infusion of JT_{ChAT} lymphocytes after with (4) L-NAME or (5) atropine. Arrows indicate the time for infusion start. The cut in the tracings indicate the period of infusion-related measurement artifacts. c) Mean MAP change from baseline x time expressed as area under the curve ± SEM is shown for mice injected with saline (n=19), JT lymphocytes (n=13) or JT_{ChAT} lymphocytes (n=9). Mice were pre-treated with L-NAME (n=7) or atropine (n=8) as indicated. * - $p<0.05$, *** - $p<0.001$ (ANOVA with Bonferroni post-hoc analysis).